BMC Structural Biology

Research article

Solution structure of the second bromodomain of Brd2 and its specific interaction with acetylated histone tails

Hongda Huang, Jiahai Zhang, Weiqun Shen, Xingsheng Wang, Jiawen Wu, Jihui Wu* and Yunyu Shi*

Address: Hefei National Laboratory for Physical Sciences at Microscale and School of Life Science, University of Science and Technology of China, Hefei, Anhui 230026, People's Republic of China

Email: Hongda Huang - hhd075@mail.ustc.edu.cn; Jiahai Zhang - zhangjh@ustc.edu.cn; Weiqun Shen - swq@ustc.edu.cn; Xingsheng Wang - wangxs05@ustc.edu.cn; Jiawen Wu - jwwu@mail.ustc.edu.cn; Jihui Wu* - wujihui@ustc.edu.cn; Yunyu Shi* - yyshi@ustc.edu.cn

* Corresponding authors

Abstract

Background: Brd2 is a transcriptional regulator and belongs to BET family, a less characterized novel class of bromodomain-containing proteins. Brd2 contains two tandem bromodomains (BD1 and BD2, 46% sequence identity) in the N-terminus and a conserved motif named ET (extra C-terminal) domain at the C-terminus that is also present in some other bromodomain proteins. The two bromodomains have been shown to bind the acetylated histone H4 and to be responsible for mitotic retention on chromosomes, which is probably a distinctive feature of BET family proteins. Although the crystal structure of Brd2 BD1 is reported, no structure features have been characterized for Brd2 BD2 and its interaction with acetylated histones.

Results: Here we report the solution structure of human Brd2 BD2 determined by NMR. Although the overall fold resembles the bromodomains from other proteins, significant differences can be found in loop regions, especially in the ZA loop in which a two amino acids insertion is involved in an uncommon π-helix, termed πD. The helix πD forms a portion of the acetyl-lysine binding site, which could be a structural characteristic of Brd2 BD2 and other BET bromodomains. Unlike Brd2 BD1, BD2 is monomeric in solution. With NMR perturbation studies, we have mapped the H4-AcK12 peptide binding interface on Brd2 BD2 and shown that the binding was with low affinity (2.9 mM) and in fast exchange. Using NMR and mutational analysis, we identified several residues important for the Brd2 BD2-H4-AcK12 peptide interaction and probed the potential mechanism for the specific recognition of acetylated histone codes by Brd2 BD2.

Conclusion: Brd2 BD2 is monomeric in solution and dynamically interacts with H4-AcK12. The additional secondary elements in the long ZA loop may be a common characteristic of BET bromodomains. Surrounding the ligand-binding cavity, five aspartate residues form a negatively charged collar that serves as a secondary binding site for H4-AcK12. We suggest that Brd2 BD1 and BD2 may possess distinctive roles and cooperate to regulate Brd2 functions. The structure basis of Brd2 BD2 will help to further characterize the functions of Brd2 and its BET members.

Background

Eukaryotic transcription is a highly regulated process. Transcription activation in eukaryotes requires the modification of histones on enhancers and promoters [1,2]. Histone acetylation plays a major role in this modification, and forms histone codes in combination with methylation, phosphorylation and ubiquitination [3-5]. One potential postulate of histone codes is that defined patterns of modification in histones can be recognized by specific factors. Bromodomain, a conserved ~110 amino acid module that is originally identified by sequence alignment as a common motif among *Drosophila* Brahma, female-sterile homeotic (fsh) and four other potential transcription regulators [6-8], can recognize acetylation of histones [9-13] and is thought to participate in deciphering the histone codes [3,14-17]. Bromodomain-containing proteins have been classified into several distinct subgroups: (i) histone acetyltransferases (HATs), including GCN5, P/CAF and TAF$_{II}$250; (ii) ATP-dependent chromatin-remodeling complexes, including Brahma, Swi2, Snf2 and Brg1; (iii) the less-characterized BET (bromodomain and extra C-terminal domain) family, which is a novel class of transcriptional regulators carrying two tandem bromodomains and an ET domain [18]. Retention on chromosomes during mitosis is likely a distinctive feature of the BET family [19-21], because proteins of other bromodomain families are displaced from chromosomes during mitosis [22,23]. There are four mammalian protein members of BET family: Brd2/Ring3 (also referred to as Fsrg1), ORFX (Fsrg2), Brd4/HUNK1 (Fsrg4), Brdt (Fsrg3).

Brd2 gene is initially identified as an open reading frame localized to the class II major histocompatibility locus on human chromosome 6p21.3 and is related to the *Drosophila* gene *female sterile homeotic* (*fsh*) [24]. The homologous genes in mouse [25], frog [26], and zebrafish [27], have been reported. Brd2 is a nuclear-localized serine-threonine kinase that has elevated activity in human leukemias [28,29]. It has been shown to synergistically transactivate cell cycle regulatory genes, including *cyclin D1*, *cyclin A*, *cyclin E* and *dihydrofolate reductase* (*dhf*), in combination with Ras or MEKK through E2Fs [30]. A murine homologue of Brd2 is contained in a mediator transcription complex that involves homologues of the yeast transcriptional regulators Med6, Med7, Rgr1, and Srb7 [31]. Later on, Brd2 is reported to associate with a transcription complex containing E2F-1, E2F-2, TBP and chromatin remodeling machines [30,32,33], and to serve as a bridge between E2F-1 and TBP [34]. Brd2 is also reported to associate with mediator subunits cyclin-dependent kinase 8 (Cdk8), thyroid receptor-associated protein 220 (TRAP220), and the Pol II large subunit (Pol II ls) [35]. Directed overexpression of Brd2 in mouse lymphocytes is found to develop B-cell lymphoma and leukemia [36]. In addition, Brd2 can interact with latent nuclear antigen (LANA) of Kaposi's sarcoma-associated herpesvirus (KSHV/HHV-8) [37]. Taken together, these reports indicate that Brd2 can serve as a transcription regulator and a contributing element in oncogenesis.

The bromodomains of Brd2 have been shown to selectively bind to histone H4 tails acetylated at Lys12 (AcK12) and to be responsible for mitotic retention on chromosomes [21]. The bromodomains are essential for transcriptional activation of important E2F-responsive genes by Brd2 through E2Fs. Bromodomain-deletion derivant of Brd2 has a high level of autophosphorylation activity and exhibits significant E2F-1 phosphorylation *in vitro* compared with wild-type [32]. It is also reported that the association of Brd2 with E2Fs, mediator components and Pol II is dependent on the presence of and is stimulated by acetylated histone H3 and H4 peptides [35]. The association with E2Fs and specific interaction with acetylated histones both establish anchor points for Brd2-containing transcription complex to *cyclin A* promoter [33]. In addition, Brd4 (another BET member) also associates with mitotic chromosomes, and tethers viral DNA to host's mitotic chromosomes [20,38]. Brd4 interacts with P-TEFb through its bromodomains and stimulates Pol II-dependent transcription [39,40]. Hence the bromodomains and their recognition of specific acetylated histones play important roles in functions of BET family members. Bromodomains of the BET family differ substantially from those of other families in amino acid sequence, despite that they share conserved hydrophobic residues in the hydrophobic core of the domain. Previous studies showed that different bromodomains have different specificities for binding to acetylated histones in living cells [21]. However, it is yet unknown the structural basis for Brd2 recognizing the specific acetylated histone code. Here, we have determined the solution structure of the second bromodomain (BD2) of Brd2 by NMR and studied its binding properties to acetylated histone H4. Comparing this structure with bromodomains from other proteins, significant differences are found in loop regions; specifically some additional secondary structures exist in Brd2 BD2. Using NMR titration experiments, the conserved hydrophobic cavity that is previously characterized in other bromodomains is found to serve as a binding site for histone H4 acetylated at K12. Through mutational analysis, we detected that the basic residues flanking the acetylated lysine of histone H4 peptides, and some resides in loop regions of Brd2 BD2 are important for their mutual recognition. Our results provide further structural and functional details aimed at revealing how Brd2 and other BET members recognize specific acetylated histone codes and thus impact transcription.

Results

Structure description

Table 1 lists the structural statistics for the 20 structures deposited in the Protein Data Bank [PDB: 2G4A]. A large, negative Lennard-Jones potential energy was observed (-360.86 ± 15.49 kcal mol^{-1}), indicating good nonbonded geometry of the structure. For the region from residue Q302 to M406, the RMSD values to the mean structure were 0.69Å for backbone atoms and 1.18 Å for all heavy atoms [see Additional file 1]. The RMSD values for the well-defined secondary structure elements were 0.58 and 1.07, respectively. In the ZA and BC loops, there was an increasing level of disorder compared with the rigid secondary elements [see Additional file 1]. A stereoview of the backbone superimposition of the final 20 structures are shown in Figure 1A.

The tertiary structure of Brd2 BD2 consists of seven distinct helices and is totally 74% helical, which is consistent with the circular dichroism prediction (data not shown). Four of the α-helices, αZ (residues 302–315), αA (residues 349–358), αB (residues 364–381) and αC (residues 387–405), are arranged in closely compact, left-handed bundle (Figure 1B) in an antiparallel manner. Crossing angles between adjacent helices αZ and αA, αZ and αC are ~30°, while those between helices αA and αB, αB and αC

are ~10–20°. Most of the slowly exchanging NH protons in 1H-2H exchange experiments were found within these regions [see Additional file 2], which indicated that protection occurred most likely by formation of hydrogen bonds here. In the long ZA loop between helices αZ and αA, there are three additional short helices: α-helices αZ' (residues 318–326) and αA' (residues 337–342), and an uncommon π-helix, termed helix πD (residue 331–335). The two helices αZ' and αA' are conserved in hsBRG1 and GCN5 bromodomains, while helix πD is also found in Brd2 BD1 [PDB: 1X0J] [41] and Brd4 BD2 [PDB: 2I8N]. The three helix structures were also confirmed by helix-typical NOEs. Besides, helix αZ' was further affirmed by 1H-2H exchange experiments. The helix αZ' is orthogonal to helices αZ and αA. Two hydrogen bonds are formed between backbone carbonyl groups of F325 and Y326 with backbone amide groups of L349 and S350, respectively, serving to cap the helix αA and help to anchor the long ZA loop. A typical 'capping box' motif in N cap [42] involving a hydrogen bond between OD1 of Asp (D348) and NH of N3 (T351) was also found to cap the helix αA. Both D348 and T351 are highly conserved in bromodomain sequences (Figure 2). Both helices αA' and πD may be quite flexible or in 'structure breath' states for ligand binding because helix αA' contacts only with helix αB (Figure 1B), helix πD has no residue interacting directly

Table 1: Structural statistics for the selected 20 structures of Brd2 BD2ª

Number of NMR restraints used in the structure calculation	
Intra-residue	563
Sequential (|i-j| = 1)	573
Medium-range (|i-j|<5)	475
Long-range (|i-j|≥5)	355
Total NOE restraints	1966
Hydrogen bonds	49
Dihedral angle restraints	146
Lennard-Jones potential energy (kcal mol-1)	-360.86 ± 15.49
RMSD from idealized covalent geometry	
Bonds (Å)	0.0010 ± 0.00002
Angles (deg)	0.2878 ± 0.0016
Impropers (deg)	0.0972 ± 0.0038
RMSD from experimental restraints	
Distance (Å)	0.0037 ± 0.0005
cdih (deg)	0.0436 ± 0.0214
Coordinate RMSD from mean (Å) residues 302 to 406	
All backbone atoms	0.69
All heavy atoms	1.18
Secondary structure elementsᵇ	
All backbone atoms	0.58
All heavy atoms	1.07
Ramachandran plot (% residues)	
Residues in most favored regions	87.0
Residues in additional allowed regions	10.3
Residues in generously allowed regions	2.5
Residues in disallowed regions	0.2

a None of the structure exhibits distance violations greater than 0.2 Å or dihedral angle violations greater than 2°.
b Residues Q302-S315, A319-Y326, H337-I342, L349-N358, A364-Y381, D387-K405.
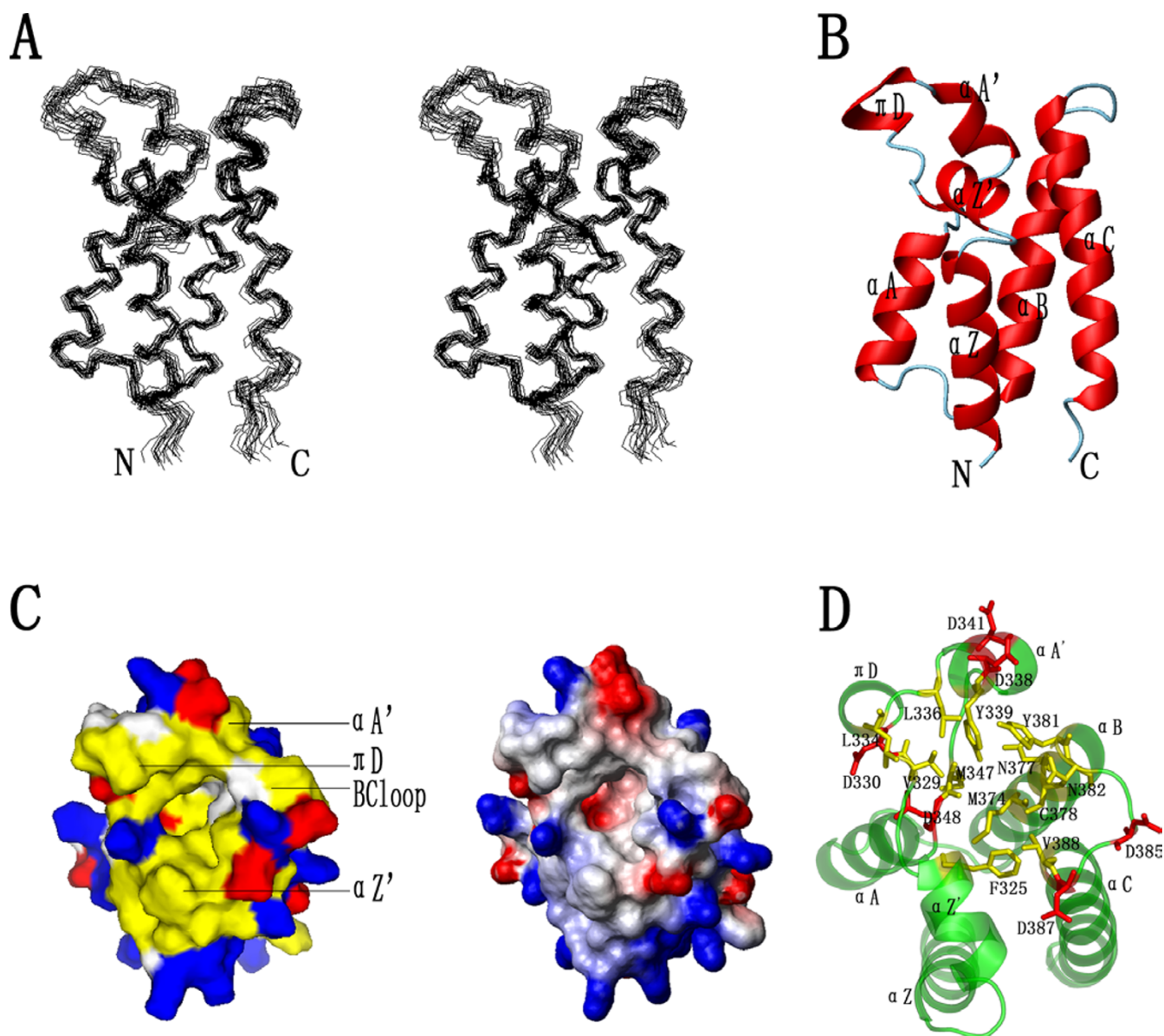
Figure 1
Structure and molecular contact surfaces of Brd2 BD2. (**A**) Stereoview of the selected 20 structures of Brd2 BD2, superimposed on backbone atoms (N, C_α and C'). (**B**) Ribbon representation of the average, energy-minimized structure with the secondary structure elements highlighted. The helix nomenclature follows that of hsP/CAF bromodomain [9]. (**C**) Contact surface emphasized surface hydrophobic potential (left) and surface electrostatic potential (right) at the acetyl-lysine binding site. Yellow denotes hydrophobic potential; red negative potential; and blue positive potential. (**D**) A clear view of showing the conserved or type conserved side chains lined the hydrophobic cavity, and denoting the negative-charged collar formed by residues D330, D338, D341, D385 and D387. A, B, C and D were produced with MOLMOL or PyMOL.

with the other helices, and few long-range NOEs and no slow-exchange NH protons are observed in these regions [43].

At the top of the protein (oriented as in Figure 1A), a groove with a cavity at the bottom could be seen clearly on the contact surface (Figure 1C). The cavity is lined by the

side-chains of residues (F325, V329, L334, L336, Y339, M347, D348, M374, N377, C378, Y381, N382 and V388) mainly from the ZA and BC loops (Figure 1D). Most of the residues are hydrophobic and highly conserved in bromodomain sequences. From surface hydrophobic potential and electrostatic potential mapping, the cavity is shown to be hydrophobic and electroneutral in nature, suitable for
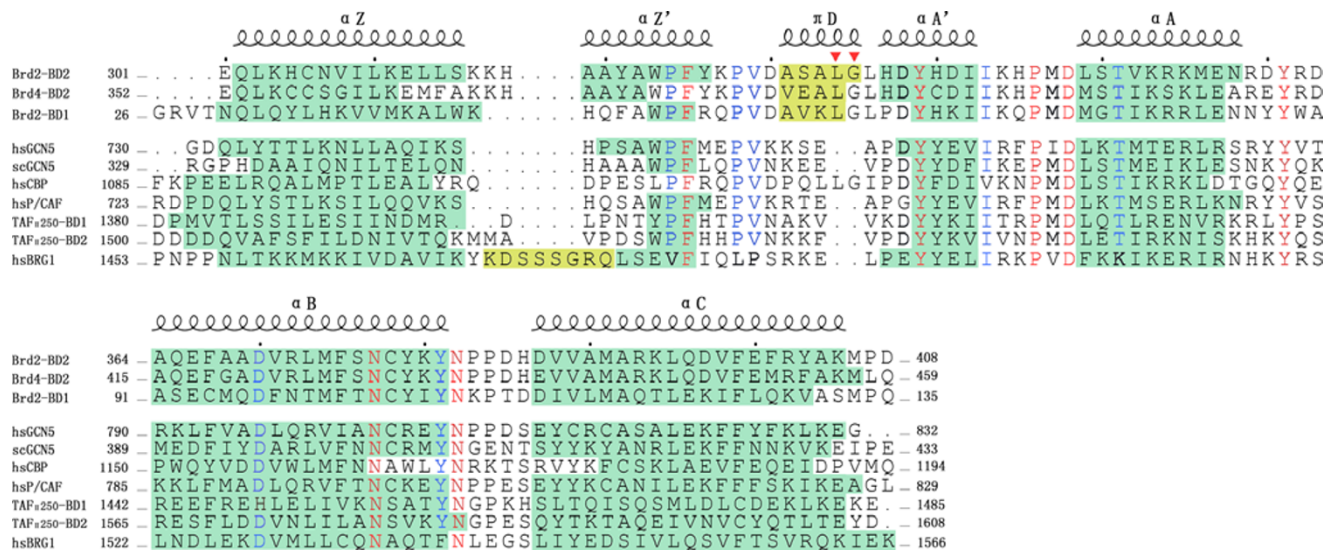
Figure 2
Sequence alignment of Brd2 BD2. Sequence alignment of Brd2 BD2 with a selected number of Bromodomains including Brd2 BD1, Brd4 BD2, hsGCN5, scGCN5, hsCBP, hsP/CAF, hsBRG1 and the two components from TAF$_{II}$250. The sequences were aligned based on the experimentally determined three-dimensional structures of these bromodomains, highlighted in green. The secondary structure of Brd2 BD2 is indicated above the alignment. Residues identical in all sequences are shown in red and residues conserved are coloured in blue and residues corresponding to βZ sheet (hsBRG1) and helix πD are represented in yellow. The two amino acids insertion is indicated by triangle symbols (▼).

hydrophobic contact mediating protein-peptide interactions. Five aspartate residues (D330, D338, D341, D385 and D387) form a negatively charged collar surrounding the edge of the hydrophobic cavity (Figure 1C and 1D). It has been proposed that these acidic residues may play a role in the specificity of bromodomain ligand binding [11].

Structure comparison with other bromodomains
In spite that Brd2 BD2 share only 22–37% sequence identity with published bromodomain structures of hsGCN5, scGCN5, hsCBP, hsP/CAF, hsBRG1, and of the double bromodomain from TAF$_{II}$250 [9,11-13,44-47], the overall secondary elements and structural fold of Brd2 BD2 resemble those published bromodomains, as shown by the backbone superposition of those structures on the average, energy-minimized structure of Brd2 BD2 (Figure 2) and [see Additional file 3]. The pairwise backbone RMSDs of those structures to Brd2 BD2 are between 1.6 to 2.6 Å. Recently, the structures of Brd2 BD1 and Brd4 BD2 (our lab unpublished data) have also been solved. Brd2 BD2 possesses high sequence identity and structural similarities to its BET members (Figure 2), with pairwise backbone RMSDs between 1.4 to 1.8 Å. Figure 3 shows the backbone superposition of Brd2 BD2 on Brd2 BD1. Our results give further evidence that the unique structural fold, especially the four-helix left-handed bundle involv-

ing helices αZ, αA, αB and αC, is highly conserved in the bromodomain family.

The majority of structural deviations are localized in the loop regions, particularly the long ZA loop. There are different additional secondary structures in the ZA loop, including helices αZ', πD and αA' (Figure 2). All the bromodomain structures solved possess helix αA', and all have helix αZ' except hsCBP. In the bromodomains of hsGCN5, hsBRG1 and Brd2 BD1 the helix αZ' is a 3_{10}-helix [11,41,46], while in Brd2 BD2 it is an α-helix defined by typical α-helical NOE and hydrogen bond patterns [see Additional file 2]. Another character of helix αZ' in Brd2 BD2 is that it is longer compared with the others. An uncommon π-helix, helix πD, is localized in the center of the ZA loop of Brd2 BD2; relevant α-helices are present in Brd2 BD1 and Brd4 BD2, but no corresponding helices are present in other bromodomain structures (Figure 2). A sequence feature of Brd2 BD2 and its BET family members is that they have a long ZA loop and a two amino acids insertion. Coincidently, the two amino acids insertion of Brd2 BD2 (L334G335) is in the helix πD and contributes to the hydrophobic groove, consequently it may play a role in ligand selectivity. The helix πD could be a structural characteristic of Brd2 BD2 and other BET bromodomains (Figure 2 and Figure 3). In the sequence of hsBRG1 bromodomain, there is also an insertion which forms a βZ
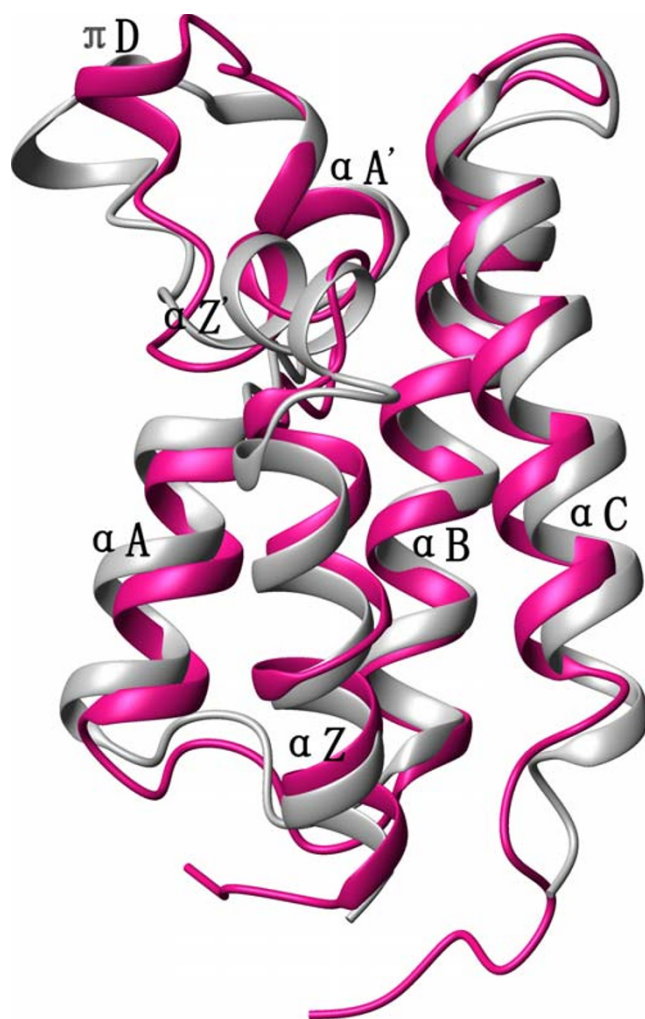
Figure 3
**Backbone superposition of Brd2 BD2 and BD1 struc-
tures**. Backbone superposition of the average, energy-mini-
mized structure of Brd2 BD2 (grey) with the crystal
structure of Brd2 BD1 (pink) [PDB: 1X0J]. The figure was
generated with MOLMOL.

sheet between helices αZ and αZ'[46]. Both the uncom-
mon helix πD in Brd2 BD2 and the βZ sheet in hsBRG1
support the view that bromodomains present in different
proteins must harbor sufficient structural diversities to
support specific recognition of acetylation codes.

Binding interface of H4-AcK12 peptide on Brd2 BD2
A previous study has demonstrated that Brd2 selectively
interacts with acetylated Lys 12 on histone H4 [21].
Accordingly, we have designed three histone tail peptides
(Table 2), H2B-AcK5, H4-AcK8 and H4-AcK12, to titrate
Brd2 BD2 using NMR experiments. The H4-AcK12 pep-
tide induced a number of distinct chemical shift perturba-
tions in the resonances of backbone amide groups of Brd2

BD2 in the ^{1}H-^{15}N HSQC spectrum (Figure 4). These
chemical shift changes increased gradually throughout the
titration that was taken to a maximum H4-AcK12 peptide:
Brd2 BD2 ratio of 10:1. These data indicate interactions
between Brd2 BD2 and H4-AcK12 peptide, and show that
the peptide and the protein are in fast exchange between
free and bound states on the NMR chemical shift times-
cale. Four most perturbed and not severely overlapped
residues, G335, L336, Y339 and Y381, were plotted in fig-
ure 4B, and the dissociation constant (K_D) for H4-AcK12
peptide was estimated to be ~2.9 mM [48]. Unlike H4-
AcK12 peptide, H4-AcK8 peptide just slightly perturbed
the chemical shifts of several residues such as G335, L336
and Y339 at very high peptide concentrations and didn't
appear to interact significantly with Brd2 BD2. Addition
of H2B AcK5 peptide resulted in little, if any, chemical
shift perturbations of any protein residue, even at high
concentrations. Totally, our titration analysis showed that
Brd2 BD2 selectively bound to H4-AcK12, which was con-
sistent with a previous report [21]; further we acquired the
K_D value for Brd2 BD2 binding to H4-AcK12 and deter-
mined this interaction to be dynamic in solution.

Additionally, our titration results made us to move for-
ward to map the binding interface of H4-AcK12 peptide
on Brd2 BD2 (Figure 5). Most residues experienced signif-
icant chemical shift changes upon addition of H4-AcK12
peptide were concentrated in the ZA and BC loop, and the
α-helical regions immediately flanking the BC loop.
Among these residues, D330, L334, G335, L336, H337,
D338, Y339, H340, D341, Y381 and A392 showed com-
bined chemical shift changes of more than the mean value
plus one standard deviation, and residues F325, A331,
H345, L373, M374, F375, Y379, N382, D385, H386,
D387, A390, M391, R393, K394, V398, K405 and M406
had combined chemical shift changes larger than mean
value. Many of the residues that were significantly dis-
turbed contribute to the hydrophobic pocket of Brd2 BD2
that serves as a primary binding surface for acetyl-lysine as
in the other bromodomains (Figure 1D) [9,11-13,44-47].

Mutational analysis
The complex structure of scGCN5 bromodomain with
H4-AcK16 peptide revealed that the major binding deter-
minant was the acetylated lysine and that the secondary
interaction came from the side chains at K+2 and K+3
positions [13]. The scGCN5 bromodomain only con-
tacted with acetylated Lys 16, His 18 (K+2) and Arg 19
(K+3). The corresponding residues in H4-AcK12 peptide
are unconserved Gly 14 (K+2) and Ala 15 (K+3) (Table 2).
We designed a set of mutations of the H4-AcK12 peptide
to determine which residues are critical for binding Brd2
BD2. NMR titrations of wild type Brd2 BD2 were per-
formed using H4-AcK12 mutant peptides, including H4-
L10A, H4-L10G, H4-A15G, H4-acid and the unacetylated

Table 2: Peptides used for binding to Brd2 BD2

Name	Sequence	Derivation
H2B-AcK5	SDPA-AcK-SAPAPKK	residues 1–12 of histone H2B
H4-AcK8	SGRGKGG-AcK-GLGK	residues 1–12 of histone H4
H4-AcK12	GKGLG-AcK-GGAKR	residues 7–17 of histone H4
H4-L10A	GKGAG-AcK-GGAKR	Leu 10 to Ala mutation of H4-AcK12
H4-L10G	GKGGG-AcK-GGAKR	Leu 10 to Gly mutation of H4-AcK12
H4-A15G	GKGLG-AcK-GGGKR	Ala 15 to Gly mutation of H4-AcK12
H4-acid	GDGLG-AcK-GGADE	Lys 8 to Asp, Lys 16 to Asp and Arg 17 to Glu mutations of H4-AcK12
H4-U	GKGLGKGGAKR	residues 7–17 of histone H4

peptide H4-U (Table 2 and Figure 6). The H4-U and H4-acid peptides did not disturb any residue amide resonances of Brd2 BD2, indicating that acetylated H4 tail was the preferred substrate and that those basic residues, Lys 8, Lys 16 and Arg 17 of H4 tail, could play an important role in the interactions. The H4-L10A and H4-L10G peptides induced small but still significant resonance shifts. The chemical shift changes induced by H4-A15G were like those in response to H4-AcK12 at a low peptide: Brd2 BD2 ratio of less than 4:1. Strikingly, when H4-A15G peptide: Brd2 BD2 ratio was large than 4:1, all the amide resonances of Brd2 BD2 disappeared. This phenomenon was confirmed by repeated titration experiments with two different protein concentrations (data not shown).

Further more, Brd2 BD2 mutants, including V329A, L334A, L336A and N382A, were titrated with the H4-AcK12 peptide, respectively. The integrity of Brd2 BD2 mutants were assessed by their ^{15}N-HSQC spectra. Compared with the ^{15}N-HSQC spectrum of Brd2 BD2, mutants V329A and N382A showed significant differences of amide resonances for residues in the ZA and BC loop, and some residues localized in the termini of helices αB and αC; mutant L336A exhibited moderate differences for residues in the ZA and BC loop; whereas mutant L334A just slightly affected vicinal residues (Figure 7) and [see Additional file 4]. Both mutants V329A and N382A showed no binding to H4-AcK12 peptide, which should be attributed to severe disruption of the conformation of the binding cavity. Mutants L334A and L336A have fewer residues perturbed upon H4-AcK12 binding than wild type Brd2 BD2, and the perturbations are smaller. The unambiguous and significantly perturbed residue G335 was followed during titrations and plotted in figure 8.

Dynamic properties of Brd2 BD2
The longitudinal relaxation times (T_1 ms), transverse relaxation times (T_2 ms) and ratio of NOE intensity are recorded to probe the dynamic properties of Brd2 BD2. The T_2 relaxation times were obtained for 85% of the backbone amide protons; the T_1 relaxation times and ^{1}H-^{15}N heteronuclear NOE values were obtained for 90% of the backbone amide protons (Figure 9). The overall rotational correlation time (τ_m) of the ~13.8-KD Brd2 BD2 is 10 ns (as estimated from the average values of T_1/T_2), suggesting that BD2 is mainly monomeric in solution. The average ^{1}H-^{15}N NOE value is 0.76 ± 0.09, indicating that most of the regions of Brd2 BD2 are relatively rigid, corresponding well with the narrow distribution of conformers in the calculated ensemble. Some residues in the ZA and BC loop have relatively lower ^{1}H-^{15}N NOE values and these two loops construct the ligand-binding groove of Brd2 BD2 (Figure 9) and [see Additional file 1].

Discussion
BET family is a less characterized novel class of bromodomain-containing proteins [18]. In the present work, we have determined the solution structure of the second bromodomain of Brd2, which shares more sequence identity with other BET bromodomains than with bromodomans of other families (Figure 2). The structure of Brd2 BD2 consists of a previously characterized four-helix left-handed bundle, with additional helices in ZA loop. Compared with other published bromodomain structures, extensive structural variations are found in loop regions (ZA and BC loop); especially, in ZA loop there exists an uncommon helix πD that is also present in BET family members Brd2 BD1 and Brd4 BD2. We speculate that the specific recognition of H4-AcK12 may involve this helix πD. Recently published structure of hsBRG1 bromodomain reveals a βZ sheet insertion between helices αZ and αZ'. The βZ sheet is proposed to have a role in orienting an acetylated substrate by changing the flexibility of the ZA loop [46]. The observations of the uncommon helix πD insertion in Brd2 BD2 and the βZ sheet insertion in hsBRG1 demonstrate that different bromodomains must have sufficient structural diversities to support specific recognition of acetylation codes. More and more information appears about the important functions of proteins in the BET family; especially that it is observed that Brd2, as well as Bdf1 and Brd4, remains mitotically associated with chromatin [19-21]. Our study provides a structural basis to further understand the functions of proteins in the BET family.
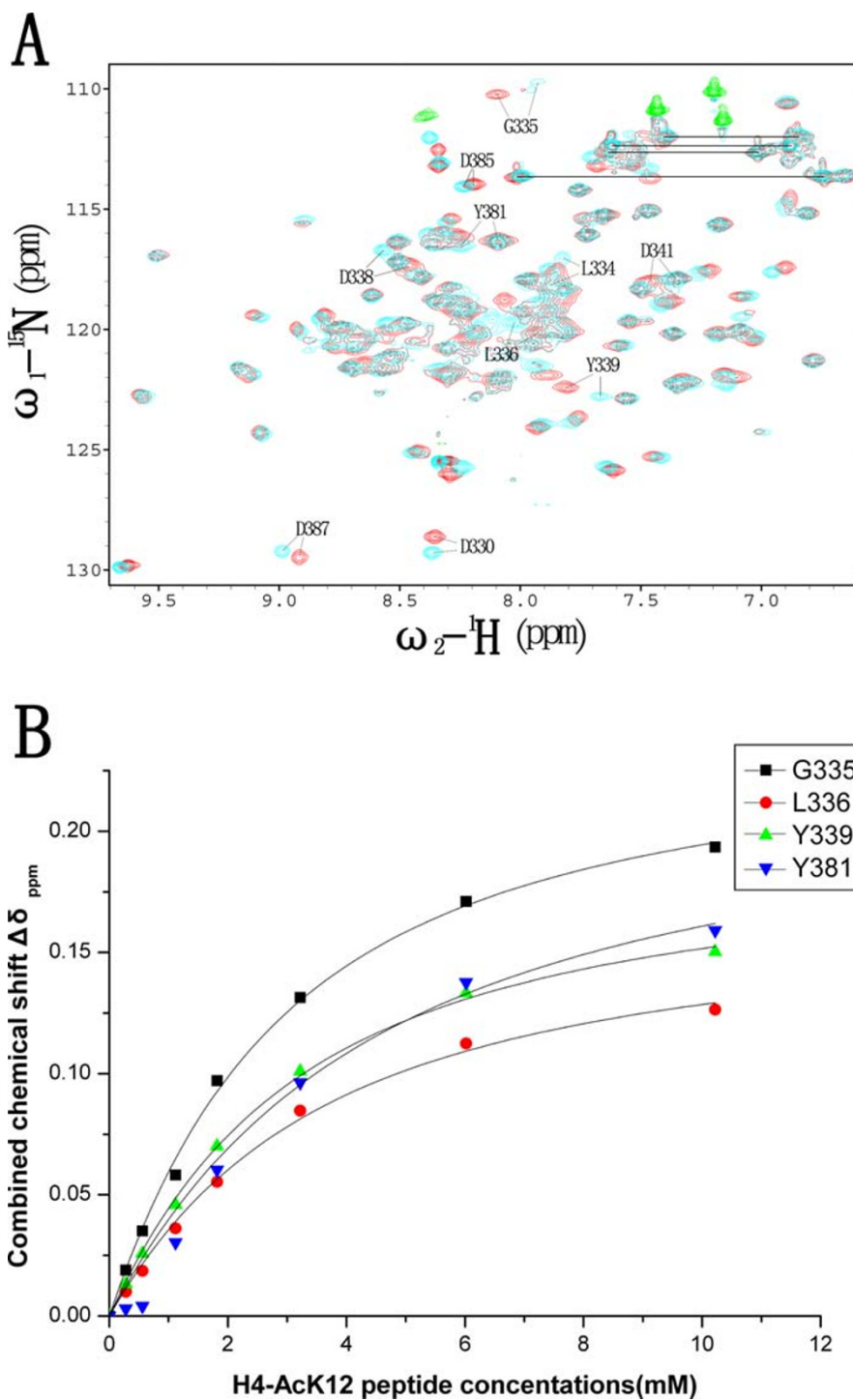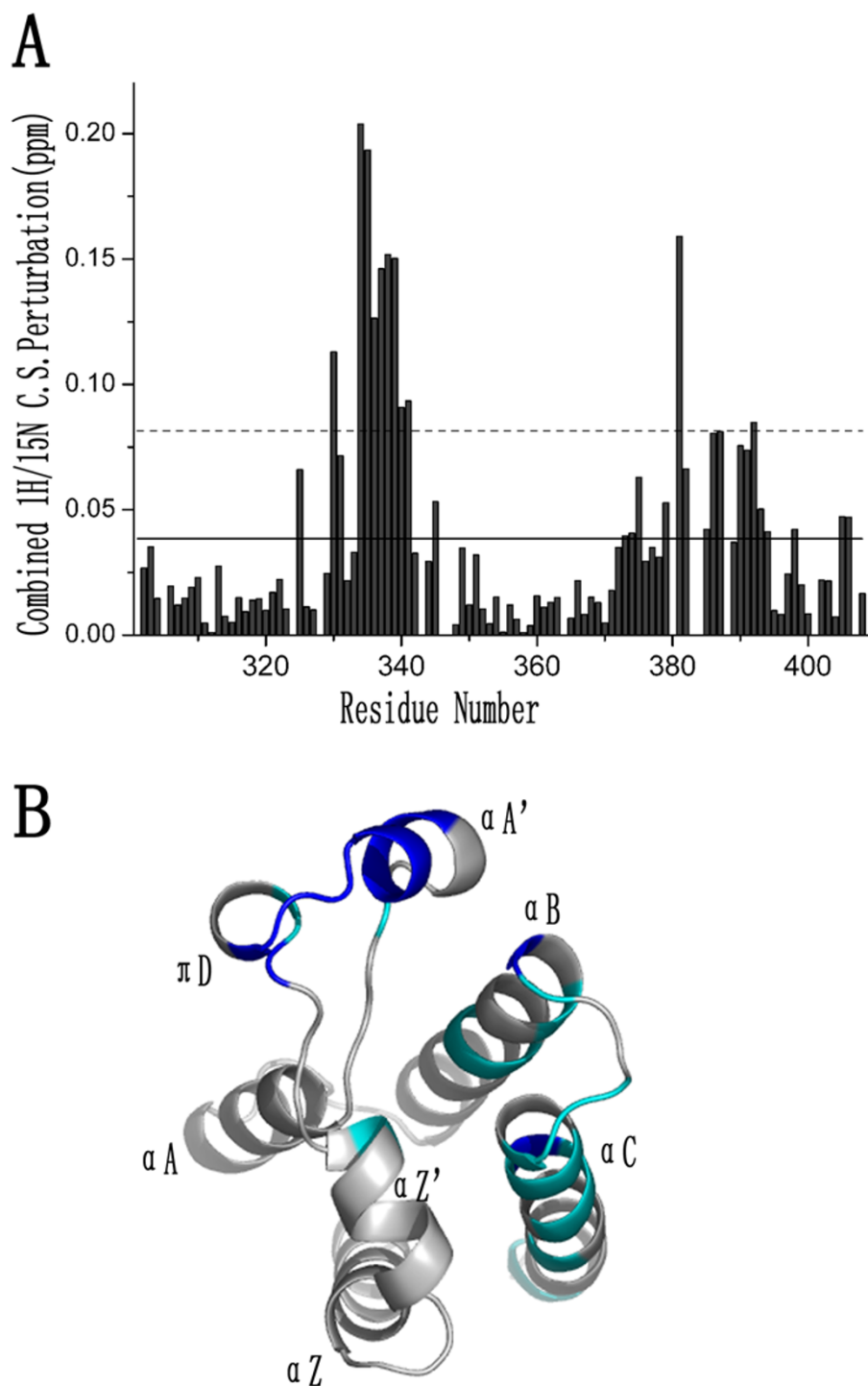
Figure 4
Analysis of the interaction of Brd2 BD2 with H4-AcK12 peptide by NMR. (**A**) Overlay of the ^{15}N-HSQC spectra of Brd2 BD2 in free of H4-AcK12 peptide (red) and in the presence of H4-AcK12 peptide (cyan). Five of the most perturbed residues (L334, G335, L336, Y339, and Y381) and the five negative-charged aspartate residues (D330, D338, D341, D385 and D387) were denoted. (**B**) Binding constant was determined by monitoring the combined chemical shift perturbations ($\Delta\delta_{ppm}$) of four most perturbed and not severely-overlapped residues (G335, L336, Y339 and Y381) as a function of concentrations of H4-AcK12 peptide.

Figure 5
Binding interface of H4-AcK12 peptide on Brd2 BD2. (**A**) A histogram view of combined chemical shift perturbations of Brd2 BD2 by addition of H4-AcK12 peptide. The mean value is denoted as a solid line and the mean value plus one standard deviation as a dash line. (**B**) A ribbon diagram view mapping the binding interface of H4-AcK12 peptide on Brd2 BD2. The residues, whose combined chemical shift changes were more than the mean value plus one standard deviation and above the mean value, are colored in blue and cyan respectively. The figure B was generated in PyMOL.
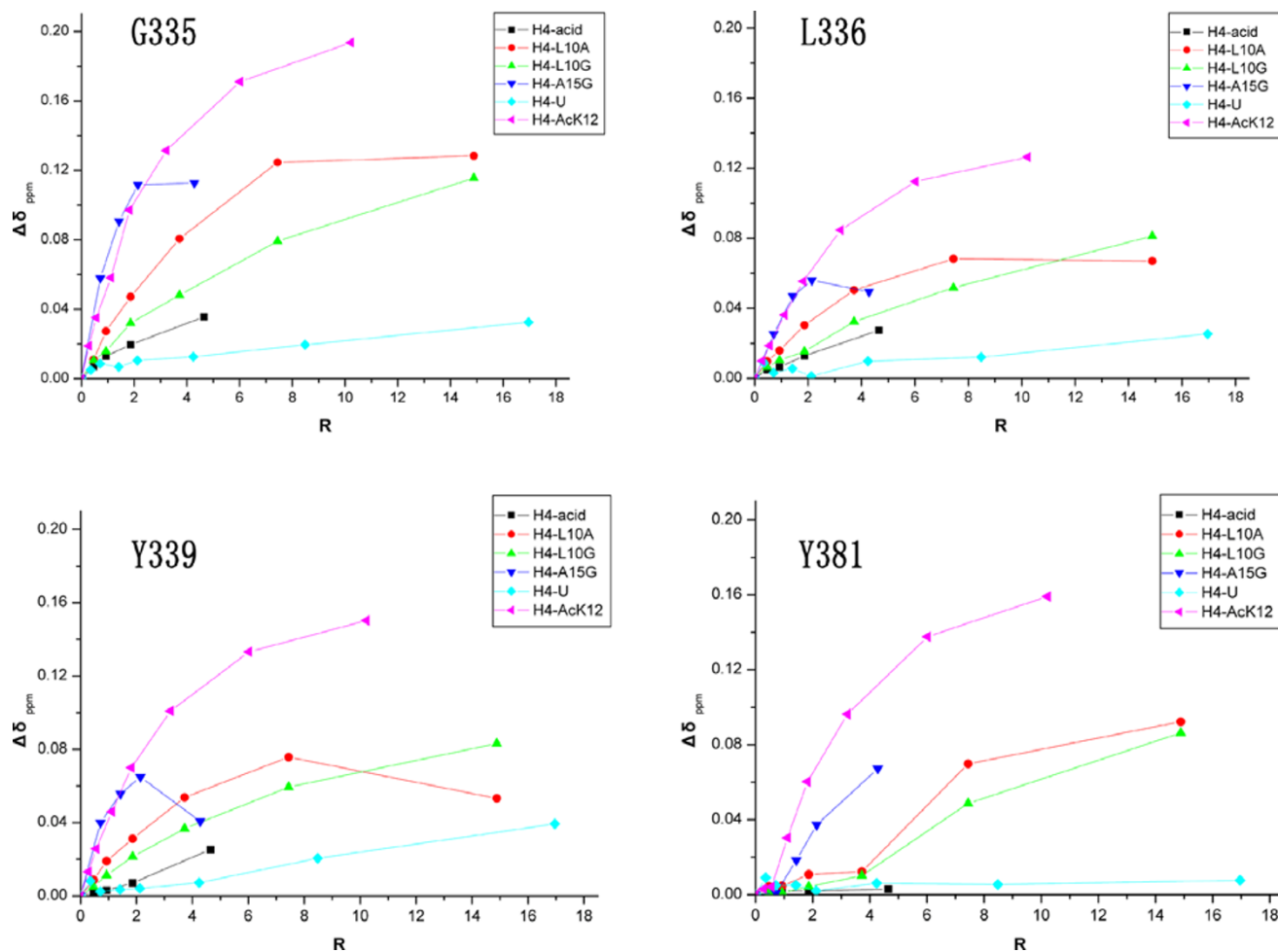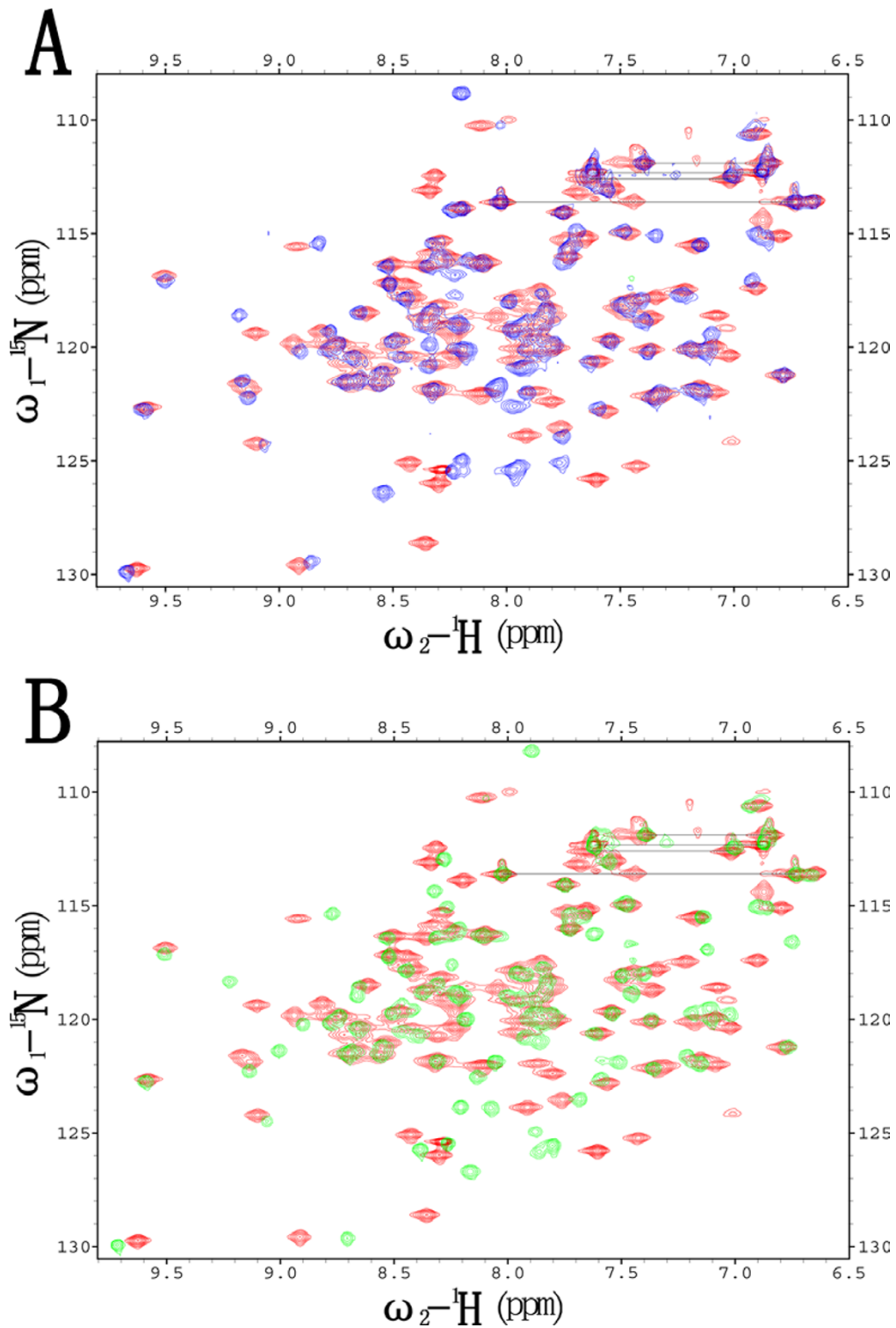
Figure 6

NMR titrations of Brd2 BD2 with mutated histone H4 tails. Brd2 BD2 was titrated with different H4-AcK12 peptide mutants, including H4-L10A, H4-L10G, H4-A15G, H4-acid and the unacetylated peptide H4-U. Combined chemical shift perturbation was calculated using the equation, $\Delta\delta_{ppm} = \sqrt{(\Delta\delta_{HN})^2 + (\Delta\delta_N \alpha_N)^2}$, and R = [peptide]/[bromodomain].

Consistent with a former study [21], our NMR titration experiments show that Brd2 BD2 specifically binds to H4-AcK12 peptide. We acquired the K_D value (2.9 mM) for this specific binding and determined the interaction to be dynamic in solution. Brd2 BD2 binds to H4-AcK8 peptide with much lower affinity and does not bind to H2B-AcK5 peptide or unacetylated peptide H4-U at all. While the full length Brd2 can bind to H2B acetylated at K5/K12 [21], Brd2 BD2 can not. One possibility is that Brd2 BD1 is responsible for this interaction. The binding interface of H4-AcK12 peptide on Brd2 BD2 is further identified by NMR titration experiments, which is a conserved hydrophobic and electroneutral cavity with a negative-charged collar formed by five aspartate residues (D330, D338, D341, D385 and D387). These aspartate residues exhib-

ited significant chemical shift changes in Brd2 BD2 titration with H4-AcK12 peptide and served as a secondary binding site as in hsGCN5 bromodomain [11]. The N-terminal tail of histone H4 is positively charged; and coincidently, when the positively charged residues (Lys 8, Lys 16 and Arg 17) flanking the acetylated lysine were mutated to negatively charged residues, Brd2 BD2 no longer bound to this peptide (Table 2 and Figure 6). When another flanking residue Ala 15 on H4-AcK12 peptide was substituted with glycine, it induced high aggregation of Brd2 BD2 with an unknown mechanism. Thus, the residue Ala 15 may also have a role in the specific recognition of H4-AcK12 by Brd2 BD2. The complex structure of scGCN5 with H4-AcK16 peptide revealed a primary interaction provided by acetylated lysine and a secondary interaction

Figure 7
Structural integrity analysis of Brd2 BD2 mutants. The integrity of Brd2 BD2 mutants were assessed by their ^{15}N-HSQC spectra. (**A**) Overlay of the ^{15}N-HSQC spectra of Brd2 BD2 (red) and V329A (blue); (**B**) Overlay of the ^{15}N-HSQC spectra of Brd2 BD2 (red) and N382A (green).
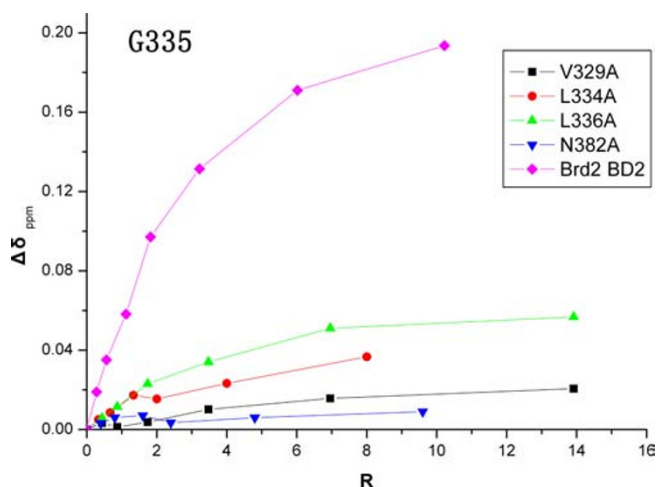
Figure 8
Plot of Brd2 BD2 mutants titrations with H4-AcK12 peptide. Brd2 BD2 mutants including V329A, L334A, L336A and N382A, were titrated with H4-AcK12 peptide. The doubtless and more significant perturbed residue G335 during titrations was followed.

came from K+2 and K+3 positions [13]. Our result of Brd2 BD2 not binding to unacetylated peptide H4-U also solidate the notion that an acetylated lysine is a determinant in bromodomain-ligand recognition. Residues Lys 8, Lys 16 and Arg 17 (corresponding to K-4, K+4 and K+5 positions) provide a secondary recognition, while the residue Ala 15 (corresponding to K+3 position) may also be involved in the interaction with Brd2 BD2. So the interaction mode for Brd2 BD2 with H4-AcK12 peptide may be different from that of scGCN5-H4-AcK16 complex, which is further supported by the observation of large sequence and structural variations in the ZA and BC loops between Brd2 BD2 and scGCN5 [see Additional file 5].

The H4-AcK12 peptide binding pocket on Brd2 BD2 is constructed of many conserved or type-conserved resides. To determine which is crucial for H4-AcK12 recognition, we designed a series of mutations in the binding cavity, including V329A, Y339F, Y339A and N382A in respect that all these corresponding residues in hsP/CAF, hsCBP or scGCN5 bromodomains have extensive contacts with their ligands. Especially, the highly conserved residue N382 may be involved in orienting the acetylated Lys 12 as its corresponding residue N407 in scGCN5 [13]. Mutant N382A was constructed to examine its effect in H4-AcK12 interaction. ^{15}N-HSQC spectra revealed that when the conserved residue V329 or N382 is mutated to alanine, the Brd2 BD2 conformation is disrupted throughout ZA and BC loops, even extending to the helices B and C for N382A mutant. Neither mutant V329A nor mutant N382A binds to H4-AcK12 peptide. For Y339F

and Y339A mutants, the recombinant proteins have converted into inclusion body when expressed in *E. coli* (data not shown). Thus these highly conserved residues may be more important in maintaining a proper conformation for ligand recognition. On the other hand, L334A or L336A mutant just mildly disturbs a few adjacent residues and most likely doesn't affect the conformation of the binding pocket. However, these two mutants bind to H4-AcK12 with much lower affinities compared with wild type Brd2 BD2. Mutation-induced function disruption may be the main reason for L334A and L336A mutants not binding to H4-AcK12 peptide. Both residues L334 and L336 are localized in helix πD (residue 331–335), and L334G335 forms a two amino acids insertion unique to Brd2 BD2 and other BET members. Our results definitely show that the two amino acids insertion and helix πD are implicated in Brd2 BD2 and H4-Ack12 peptide interaction. However, the complex structure of Brd2 BD2 with H4 AcK12 peptide is needed to completely understand the interaction mechanism.

The solution structure of Brd2 BD2 is monomeric, whereas the crystal structure of Brd2 BD1 is determined to be a homodimer [41]. No inter-molecular NOEs were observed in Brd2 BD2, which was consistent with monomeric state as indicated by gel-filtration and GST-pull down analysis (see methods). It is not surprising that Brd2 BD1 shares only 46% sequence identity with BD2 and the dimeric residues are just partially conserved in BD2. In fact, the equivalent BD1s or BD2s from different proteins of BET family share higher homologies than the non-equivalent BD1 and BD2 in the same protein. Although both Brd2 BD1 and BD2 specifically recognize the same acetylated histone H4 tail, it is reasonable to propose that they play distinctive roles in Brd2 functions. In the Brd2 containing coactivator complex, BD1 may be a dimeric module and interacts with TBP [33], while BD2 may mainly serve to bind to acetylated histones. It is also probable that Brd2 BD1 and BD2 interact with acetylated histones in different context. And multi-bromodomains could enhance the affinity for acetylated histones. An intriguing question immediately rises and waits to answer. How Brd2 BD1 and BD2 cooperate to regulate Brd2 functions, and thus modulate its transcriptional activation effect?

Conclusion
Brd2 BD2 is monomeric in solution and interacts weakly and dynamically but specifically with H4-AcK12. The helix πD in the long ZA loop may be a common characteristic of BET bromodomains. The conserved hydrophobic cavity is found to serve as a primary binding site for H4-AcK12 as in other bromodomains. A negatively charged collar of the cavity serves as a secondary binding site for H4-AcK12. Actually, the flanking basic residues on H4-
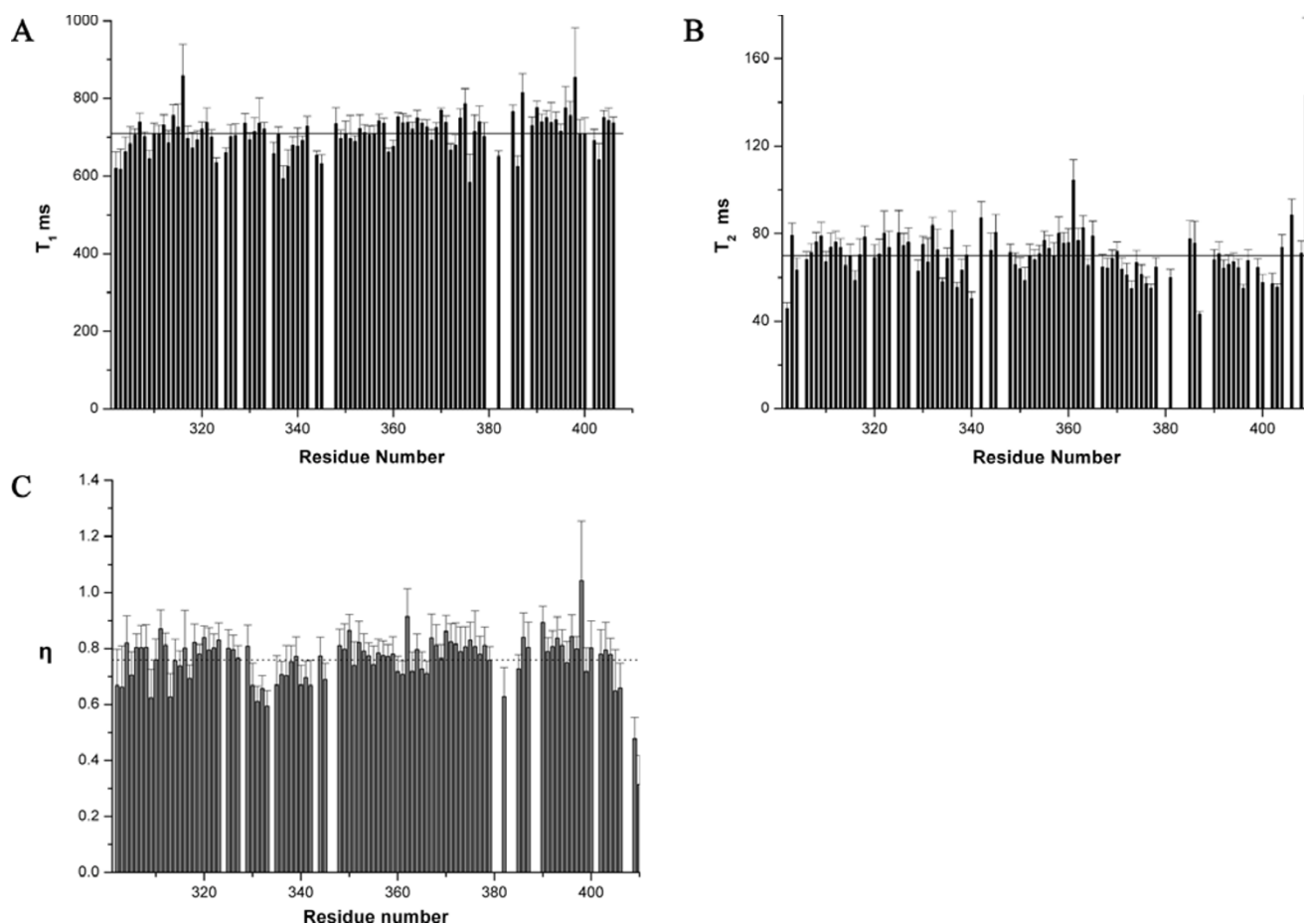
Figure 9
Plot of the longitudinal and transverse relaxation times and ratio of intensity of NOE. The longitudinal (T_1 ms) (**A**) and transverse relaxation times (T_2 ms) (**B**) and ratio of intensity of NOE (**C**) are plotted as a function of residue number of Brd2 BD2. Only those residues of which ^1H-^{15}N cross-peaks are resolved enough to permit accurate measurements of their intensities are included.

AcK12 are important for their mutual recognition. Brd2 BD1 and BD2 may cooperate to regulate Brd2 functions. The structure of Brd2 BD2 will help to further characterize BET family members.

Methods

Cloning, expression and purification of Brd2

The DNA fragment encoding residues 301–408 corresponding to the second bromodomain of Brd2 was amplified from human brain cDNA library (Clontech) by a polymerase chain reaction (PCR) using the two primers 5'-CTCGAGATCTGGCATCTTGGCATAACGG-3' and 5'-CATATGGAACAGTTAAAACATTGCAATG-3' (restriction sites are underlined) designed based on the mRNA sequence of Brd2 [GenBank: M80613]. The reaction product (about 330 bp) was purified and then cloned into pGEM-T vector (Promega). The positive clones were identified by restriction digest. Then the DNA fragment was

ligated into the *Nde*I/*Xho*I-cleaved plasmid pET22b(+) (Novagen), yielding plasmid pET22b-BD2. The plasmid pET22b-BD2 was then transformed into *Escherichia coli* BL21 (DE3) host cells for expression. Uniformly labeled recombinant Brd2 BD2 was produced using SV40 medium containing 0.5 g/l 99% ^{15}N ammonium chloride and 2.5 g/l 99% ^{13}C-glucose as the sole nitrogen and carbon source, respectively. Recombinant Brd2 BD2 was purified using Ni-chelating column (Qiagen). The purified recombinant Brd2 BD2 protein contains a C-terminal His tag (LEHHHHHH), with the N-terminal Met cleaved during expression (data from Mass spectrum). The purity of recombinant Brd2 BD2 was confirmed by Tricine-SDS-PAGE (15%, w/v) and the concentration was measured with BCA kits (Pierce). The ^{15}N-labeled and ^{13}C, ^{15}N-labeled Brd2 BD2 were about 0.5–1.0 mM. All the samples for NMR contained 50 mM phosphate buffer (pH 5.8), 50 mM NaCl, 1 mM DTT, 1 mM EDTA in 90% H_2O/

10% D_2O or in 99.96% D_2O. Brd2 BD2 mutants were generated by conventional PCR method using pET22b-BD2 plasmid as template. Mutants V329A, L334A, L336A and N382A represented mutations of Val 329 to Ala, Leu 334 to Ala, Leu 336 to Ala and Asn 382 to Ala respectively. The uniformly ^{15}N-labled proteins of Brd2 BD2 mutants were produced as described above. The integrity of Brd2 BD2 mutants were assessed by their ^{15}N-HSQC spectra.

For GST fusion Brd2 BD2, the DNA fragment was cloned into pGEX-4T (Amersham Bioscience) resulting plasmid pGEX-BD2. The construct was also expressed in *Escherichia coli* BL21 (DE3). The GST fusion protein was purified using Sepharose 4B (Amersham Bioscience) and following the protocols.

Characterization of Brd2 BD2 in solution
The state of purified recombinant His-tagged Brd2 BD2 in solution was analyzed using gel filtration chromatography and GST-pull down experiments. The gel filtration analysis was performed with a ÄKTA FPLC instrument (Amersham Biosciences) equipped with Hiload 16/60 Superdex 75 prep grade column. The purified His-tag fusion Brd2 BD2 was loaded onto the column equilibrated with a buffer containing 50 mM Tris and 500 mM NaCl (pH7.8) and was eluted with the same buffer. The molecular weight was calibrated with marker proteins included Cytochrome C (MW 12300), Myoglobin (horse, MW 17800), Chymotrypsinogen (MW, 25000), Albumin (egg, MW 45000), Albumin (bovine serum, MW 67000). In the analysis, Brd2 BD2 was eluted as a single peak, demonstrating the homogeneity of the sample. The apparent molecular weight of Brd2 BD2 was estimated to be 11 KD, corresponding well with the theoretic molecular weight of Brd2 BD2 (13.8 KD) (data not shown).

In GST-pull down experiments, the purified recombinant GST and GST-BD2 were immobilized on 200 μl Sepharose 4B beads. After washing four times (1 ml every time) with GST binding buffer, the beads were then incubated with excessive amount of His-tag fusion Brd2 BD2 in total volume of 1 ml at 4°C overnight. The beads were washed by GST binding buffer supplemented with different concentrations of NaCl. Finally the proteins were eluted from beads by boiling. All samples were analyzed on Tricine-SDS-PAGE (15%, w/v) and stained with Coomassie brilliant blue. The GST-pull down experiments exhibited that the His-tagged and GST-tagged Brd2 BD2 didn't associate with each other in solution (data not shown). Accordingly, the recombinant Brd2 BD2 was homogenous and mainly monomeric in solution. Hence we moved forward to perform NMR experiments of Brd2 BD2.

NMR spectroscopy and data processing
The NMR experiments were performed on a Bruker DMX600 spectrometer with self-shielded z-axis gradients. The following spectra were recorded at 298 K to obtain backbone and side chain resonance assignments: 2D ^{1}H, ^{15}N-HSQC, 2D ^{1}H, ^{13}C-HSQC, 3D triple-resonance spectra HNCO, HN(CA)CO, CBCA(CO)NH, CBCANH, C(CO)NH-TOCSY, H(CCO)NH-TOCSY, ^{15}N-TOCSY, HBHA(CBCACO)NH, 2D CB(CC)HD-COSY (aromatics), 3D ^{15}N-separted NOESY (mixing time 110 ms). The ^{13}C/^{15}N-labeled sample was then lyophilized and dissolved in 99.96% D_2O, which was followed immediately with HSQC experiments to monitor the disappearance of NH signals at 293 K. After all of the peaks vanished, 3D HCCH-TOCSY, HCCH-COSY and ^{13}C-separated NOESY (mixing time 130 ms) were recorded on this sample at 298 K.

NMR data processing was carried out using NMRPipe and NMRDraw software, and the data were analyzed with SPARKY. All software was run on a Linux system. Linear prediction was used to improve spectral resolution in the indirect dimensions where constant-time acquisition was used.

Experimental restraints and NMR structure determination
NMR distance restraints were collected from two different NOESY spectra: 3D ^{15}N-separated NOESY in H_2O for amide protons, 3D ^{13}C-separated NOESY in D_2O for aliphatic protons. NOE restraints were grouped into four distance ranges: strong, 1.8–3.0 Å and 1.8–3.5 Å; medium, 1.8–4.0 Å and 1.8–4.5 Å; weak, 1.8–5.0 Å; and very weak, 1.8–6.0 Å. Considering that the spin diffusion effect could be serious for aliphatic protons, a more conservative distance estimation was used for the 3D ^{13}C-separated NOESY; therefore, most medium-range and long-range NOEs from this spectra were put into the weak or very weak groups. The 1.8 Å lower limits were imposed only implicitly by the van der Waals repulsion force. For methyl protons, nonstereospecifically assigned methylene protons, and aromatic ring protons, r^{-6} summation averages were applied. Based on the chemical shifts values, the program CSI and TALOS were used to identify the secondary structure elements. The derived secondary structures were converted into restraints on φ and ψ angles. Hydrogen bond restraints were obtained by identifying the slow exchange amide protons mainly in the regular secondary structures.

Structures were calculated using the program CNS v1.1, employing a simulated annealing protocol for torsion angle dynamics. For the initial rounds of structure calculations, only sequential, intraresidual, medium-range NOEs, unambiguous long-range NOEs and dihedral angle restraints were used. Later, all other long-range NOEs and

hydrogen bonds were introduced in consecutive steps. Simple impulsion nonbonded interactions were used during structure calculation. At the final stage, 200 conformers were calculated; of these, 20 conformers with the lowest energy were selected. The coordinates of the 20 selected structures and the mean structure have been deposited in the Protein Data Bank [PDB: 2G4A]. The qualities of the structures were assessed with PROCHECK. All residues are located in allowed regions on Ramachandran plot apart from K217 due to paucity of inter-residual NOEs. Being unassigned, the C-terminal His tag had no NMR restraints, and they were excluded from structure calculation.

Histone N-terminal tail peptides and NMR titration

The peptides of acetylated histone tails H2B-AcK5 (residues 1–12 of histone H2B, SDPA-AcK-SAPAPKK, where AcK is an N$^\varepsilon$-acetyl-lysine), H4-AcK8 (residues 1–12 of histone H4, SGRGKGG-AcK-GLGK), H4-AcK12 (residues 7–17 of histone H4, GKGLG-AcK-GGAKR), H4-L10A (Leu 10 to Ala mutation of H4-AcK12, GKGAG-AcK-GGAKR), H4-L10G (Leu 10 to Gly mutation of H4-AcK12, GKGGG-AcK-GGAKR), H4-A15G (Ala 15 to Gly mutation of H4-AcK12, GKGLG-AcK-GGGKR), H4-acid (Lys 8 to Asp, Lys 16 to Asp and Arg 17 to Glu mutations of H4-AcK12, GDGLG-AcK-GGADE) and the unacetylated peptide H4-U (residues 7–17 of histone H4, GKGLGKGGAKR) were purchased from Sangon. All these compounds were used without additional purification. For binding titrations, the samples of ^{15}N-labeled Brd2 BD2 and Brd2 BD2 mutants were prepared in phosphate buffer (pH 5.8) as mentioned above, with the concentrations between 0.2 mM and 1.0 mM. Solutions of the peptides H2B-AcK5, H4-AcK8, H4-AcK12, H4-L10A, H4-L10G, H4-A15G, H4-U and H4-acid were prepared at concentrations between 55 mM and 100 mM, under identical buffer conditions. The ^{1}H and ^{15}N resonance variations were followed at 298 K by collecting HSQC experiments. Combined chemical shift perturbation was calculated using this equation,

$$\Delta\delta_{ppm} = \sqrt{(\Delta\delta_{HN})^2 + (\Delta\delta_N \alpha_N)^2}$$, with a scaling factor

(α_N) of 0.17.

^{15}N relaxation experiments of Brd2 BD2

The ^{15}N relaxation experiments were performed at 298 K on a Bruker DMX500 spectrometer. ^{15}N T_1 and T_2 relaxation rates with one second recycle delay were measured with eight relaxation delays (21.2, 61.4, 142, 242, 363, 523, 804, and 1210 ms) and six relaxation delays (17.6, 35.2, 52.8, 70.4, 105.6, and 140.8 ms) respectively. The spectra for measuring ^{1}H-^{15}N NOE were performed with a two seconds relaxation delay followed by a three seconds

period of proton saturation. And the spectra acquired without proton saturation employed a five seconds relaxation delay. The data analysis and exponential curve fitting were processed using SPARKY.

Abbreviations

BET, Bromodomain protein with Extra C-Terminal domain; Brd2, bromodomain containing 2; Brd2 BD1/BD2, the first/second bromodomain of Brd2; NOE, nuclear Overhauser effect; NOESY, nuclear Overhauser enhancement spectroscopy; COSY, correlated spectroscopy; TOCSY, total correlation spectroscopy; HSQC, heteronuclear single quantum correlation; RMSD, root mean square deviation.

Authors' contributions

HDH designed and carried out the experiments, drafted and revised the manuscript; JHZ helped to conceive and carry out the structural experiments; WQS helped to draft and revise the manuscript; XSW participated in preparation of the figures and revised the manuscript; JWW participated in preparation of the figures; JHW designed the experiments, carried out the structural experiments and revised the manuscript; YYS designed the experiments and revised the manuscript. All authors have read and approved the final manuscript.

Additional material

> **Additional file 1**
> *Plots of NOE restraints and RMSD.* **(A)** *Plot of the number of NOE restraints per residue used in the calculation of the Brd2 BD2 structure.* **(B)** *Plot of backbone atoms and all heavy atoms average RMSD values from the mean structure of the final ensemble of 20 structures* vs. *the sequence of Brd2 BD2.*
> Click here for file
> [http://www.biomedcentral.com/content/supplementary/1472-6807-7-57-S1.pdf]

> **Additional file 2**
> *Summary of sequential and medium-range NOE patterns. The data are derived from ^{15}N-separated and ^{13}C-separated NOESY spectra of Brd2 BD2. The thickness of the bars of sequential NOEs indicates the relative intensities of the corresponding cross-peaks in NOESY, and horizontal lines indicate the observation of medium-range NOEs between residue pairs. Filled circles denote the locations of slowly exchanging amide protons. The short bars at the bottom represent consensus CSI predictions from Cα, Cβ, C', and Hα chemical shifts; bars below the line mean an index of -1, while those above the line mean an index of +1. Four or more consecutive bars of -1 not interrupted by a bar of +1 indicate α-helix. Three or more consecutive bars of +1 not interrupted by a bar of -1 indicate β-strand.*
> Click here for file
> [http://www.biomedcentral.com/content/supplementary/1472-6807-7-57-S2.pdf]

Additional file 3

Backbone superposition of the experiment-derived bromodomain structures. (A) Backbone superposition of the average, energy-minimized structures of Brd2 BD2 (grey) with hsGCN5 (cyan); (B) Brd2 BD2 (grey) with scGCN5 (yellow); (C) Brd2 BD2 (grey) with hsCBP (magenta); (D) Brd2 BD2 (grey) with hsP/CAF (purple); (E) Brd2 BD2 (grey) and the two bromodomains from TAF$_{II}$250 (red and green); (F) Brd2 BD2 (grey) with hsBRG1 (orange). The figure was generated with MOLMOL.
Click here for file
[http://www.biomedcentral.com/content/supplementary/1472-6807-7-57-S3.pdf]

Additional file 4

Table summarization of Brd2 BD2 mutants. The integrity of Brd2 BD2 mutants including V329A, L334A, L336A and N382A, were assessed by their ^{15}N-HSQC spectra. The table lists the statistics of amide resonances disturbed by mutations.
Click here for file
[http://www.biomedcentral.com/content/supplementary/1472-6807-7-57-S4.pdf]

Additional file 5

Structural variations in the ZA and BC loops. An enlarge view of the structural variations in the ZA and BC loops between Brd2 BD2 (grey) and scGCN5 (cyan). A stick model showed the H4-AcK16 peptide of the scGCN5 complex structure.
Click here for file
[http://www.biomedcentral.com/content/supplementary/1472-6807-7-57-S5.pdf]

References

1. Peterson CL, Workman JL: **Promoter targeting and chromatin remodeling by the SWI/SNF complex.** *Curr Opin Genet Dev* 2000, **10(2):**187-192.
2. Hassan AH, Neely KE, Vignali M, Reese JC, Workman JL: **Promoter targeting of chromatin-modifying complexes.** *Front Biosci* 2001, **6:**D1054-1064.
3. Strahl BD, Allis CD: **The language of covalent histone modifications.** *Nature* 2000, **403(6765):**41-45.
4. Turner BM: **Histone acetylation and an epigenetic code.** *Bioessays* 2000, **22(9):**836-845.
5. Turner BM: **Cellular memory and the histone code.** *Cell* 2002, **111:**285-291.
6. Haynes SR, Dollard C, Winston F, Beck S, Trowsdale J, Dawid IB: **The bromodomain: a conserved sequence found in human, Drosophila and yeast proteins.** *Nucleic Acids Res* 1992, **20(10):**2603.
7. Jeanmougin F, Wurtz JM, Le Douarin B, Chambon P, Losson R: **The bromodomain revisited.** *Trends Biochem Sci* 1997, **2(5):**151-153.
8. Tamkun JW, Deuring R, Scott MP, Kissinger M, Pattatucci AM, Kaufman TC, Kennison JA: **brahma: a regulator of Drosophila homeotic genes structurally related to the yeast transcriptional activator SNF2/SWI2.** *Cell* 1992, **68(3):**561-572.
9. Dhalluin C, Carlson JE, Zeng L, He C, Aggarwal AK, Zhou MM: **Structure and ligand of a histone acetyltransferase bromodomain.** *Nature* 1999, **399(6735):**491-496.
10. Ornaghi P, Ballario P, Lena AM, Gonzalez A, Filetici P: **The bromodomain of Gcn5p interacts in vitro with specific residues in the N terminus of histone H4.** *J Mol Biol* 1999, **287(1):**1-7.
11. Hudson BP, Martinez-Yamout MA, Dyson HJ, Wright PE: **Solution structure and acetyl-lysine binding activity of the GCN5 bromodomain.** *J Mol Biol* 2000, **304(3):**355-370.
12. Jacobson RH, Ladurner AG, King DS, Tjian R: **Structure and function of a human TAFII250 double bromodomain module.** *Science* 2000, **288(5470):**1422-1425.
13. Owen DJ, Ornaghi P, Yang JC, Lowe N, Evans PR, Ballario P, Neuhaus D, Filetici P, Travers AA: **The structural basis for the recognition of acetylated histone H4 by the bromodomain of histone acetyltransferase gcn5p.** *Embo J* 2000, **19(22):**6141-6149.
14. Winston F, Allis CD: **The bromodomain: a chromatin-targeting module?** *Nat Struct Biol* 1999, **6(7):**601-604.
15. Jenuwein T, Allis CD: **Translating the histone code.** *Science* 2001, **293(5532):**1074-1080.
16. Agalioti T, Chen G, Thanos D: **Deciphering the transcriptional histone acetylation code for a human gene.** *Cell* 2002, **111(3):**381-392.
17. Loyola A, Almouzni G: **Bromodomains in living cells participate in deciphering the histone code.** *Trends Cell Biol* 2004, **14(6):**279-281.
18. Florence B, Faller DV: **You bet-cha: a novel family of transcriptional regulators.** *Front Biosci* 2001, **6:**D1008-1018.
19. Chua P, Roeder GS: **Bdf1, a yeast chromosomal protein required for sporulation.** *Mol Cell Biol* 1995, **15(7):**3685-3696.
20. Dey A, Ellenberg J, Farina A, Coleman AE, Maruyama T, Sciortino S, Lippincott-Schwartz J, Ozato K: **A bromodomain protein, MCAP, associates with mitotic chromosomes and affects G(2)-to-M transition.** *Mol Cell Biol* 2000, **20(17):**6537-6549.
21. Kanno T, Kanno Y, Siegel RM, Jang MK, Lenardo MJ, Ozato K: **Selective recognition of acetylated histones by bromodomain proteins visualized in living cells.** *Mol Cell* 2004, **13(1):**33-43.
22. Muchardt C, Reyes JC, Bourachot B, Leguoy E, Yaniv M: **The hbrm and BRG-1 proteins, components of the human SNF/SWI complex, are phosphorylated and excluded from the condensed chromosomes during mitosis.** *Embo J* 1996, **15(13):**3394-3402.
23. Kruhlak MJ, Hendzel MJ, Fischle W, Bertos NR, Hameed S, Yang XJ, Verdin E, Bazett-Jones DP: **Regulation of global acetylation in mitosis through loss of histone acetyltransferases and deacetylases from chromatin.** *J Biol Chem* 2001, **276(41):**38307-38319.
24. Beck S, Hanson I, Kelly A, Pappin DJ, Trowsdale J: **A homologue of the Drosophila female sterile homeotic (fsh) gene in the class II region of the human MHC.** *DNA Seq* 1992, **2(4):**203-210.
25. Taniguchi Y, Matsuzaka Y, Fujimoto H, Miyado K, Kohda A, Okumura K, Kimura M, Inoko H: **Nucleotide sequence of the ring3 gene in the class II region of the mouse MHC and its abundant expression in testicular germ cells.** *Genomics* 1998, **51(1):**114-123.
26. Salter-Cid L, Du Pasquier L, Flajnik M: **RING3 is linked to the Xenopus major histocompatibility complex.** *Immunogenetics* 1996, **44(5):**397-399.
27. Takami K, Zaleska-Rutczynska Z, Figueroa F, Klein J: **Linkage of LMP, TAP, and RING3 with Mhc class I rather than class II genes in the zebrafish.** *J Immunol* 1997, **159(12):**6052-6060.
28. Rachie NA, Seger R, Valentine MA, Ostrowski J, Bomsztyk K: **Identification of an inducible 85-kDa nuclear protein kinase.** *J Biol Chem* 1993, **268(29):**22143-22149.
29. Denis GV, Green MR: **A novel, mitogen-activated nuclear kinase is related to a Drosophila developmental regulator.** *Genes Dev* 1996, **10(3):**261-271.
30. Denis GV, Vaziri C, Guo N, Faller DV: **RING3 kinase transactivates promoters of cell cycle regulatory genes through E2F.** *Cell Growth Differ* 2000, **11(8):**417-424.
31. Jiang YW, Veschambre P, Erdjument-Bromage H, Tempst P, Conaway JW, Conaway RC, Kornberg RD: **Mammalian mediator of transcriptional regulation and its possible role as an end-point of signal transduction pathways.** *Proc Natl Acad Sci USA* 1998, **95(15):**8538-8543.

32. Sinha A, Faller DV, Denis GV: **Bromodomain analysis of Brd2-dependent transcriptional activation of cyclin A.** *Biochem J* 2005, **387(Pt 1):**257-269.
33. Denis GV, McComb ME, Faller DV, Sinha A, Romesser PB, Costello CE: **Identification of transcription complexes that contain the double bromodomain protein Brd2 and chromatin remodeling machines.** *J Proteome Res* 2006, **5(3):**502-511.
34. Peng J, Dong W, Chen L, Zou T, Qi Y, Liu Y: **Brd2 is a TBP-associated protein and recruits TBP into E2F-1 transcriptional complex in response to serum stimulation.** *Mol Cell Biochem* 2006.
35. Crowley TE, Kaine EM, Yoshida M, Nandi A, Wolgemuth DJ: **Reproductive cycle regulation of nuclear import, euchromatic localization, and association with components of Pol II mediator of a mammalian double-bromodomain protein.** *Mol Endocrinol* 2002, **16(8):**1727-1737.
36. Greenwald RJ, Tumang JR, Sinha A, Currier N, Cardiff RD, Rothstein TL, Faller DV, Denis GV: **E mu-BRD2 transgenic mice develop B-cell lymphoma and leukemia.** *Blood* 2004, **103(4):**1475-1484.
37. Platt GM, Simpson GR, Mittnacht S, Schulz TF: **Latent nuclear antigen of Kaposi's sarcoma-associated herpesvirus interacts with RING3, a homolog of the Drosophila female sterile homeotic (fsh) gene.** *J Virol* 1999, **73(12):**9789-9795.
38. You J, Croyle JL, Nishimura A, Ozato K, Howley PM: **Interaction of the bovine papillomavirus E2 protein with Brd4 tethers the viral DNA to host mitotic chromosomes.** *Cell* 2004, **117(3):**349-360.
39. Yang Z, Yik JH, Chen R, He N, Jang MK, Ozato K, Zhou Q: **Recruitment of P-TEFb for stimulation of transcriptional elongation by the bromodomain protein Brd4.** *Mol Cell* 2005, **19(4):**535-545.
40. Jang MK, Mochizuki K, Zhou M, Jeong HS, Brady JN, Ozato K: **The bromodomain protein Brd4 is a positive regulatory component of P-TEFb and stimulates RNA polymerase II-dependent transcription.** *Mol Cell* 2005, **19(4):**523-534.
41. Nakamura Y, Umehara T, Nakano K, Jang MK, Shirouzu M, Morita S, Uda-Tochio H, Hamana H, Terada T, Adachi N, Matsumoto T, Tanaka A, Horikoshi M, Ozato K, Padmanabhan B, Yokoyama S: **Crystal structure of the human BRD2 bromodomain: Insights into dimerization and recognition of acetylated histone h4.** *J Biol Chem* 2007, **282(6):**4193-4201.
42. Aurora R, Rose GD: **Helix capping.** *Protein Sci* 1998, **7(1):**21-38.
43. Ottiger M, Zerbe O, Guntert P, Wuthrich K: **The NMR solution conformation of unliganded human cyclophilin A.** *J Mol Biol* 1997, **272(1):**64-81.
44. Mujtaba S, He Y, Zeng L, Farooq A, Carlson JE, Ott M, Verdin E, Zhou MM: **Structural basis of lysine-acetylated HIV-1 Tat recognition by PCAF bromodomain.** *Mol Cell* 2002, **9(3):**575-586.
45. Mujtaba S, He Y, Zeng L, Yan S, Plotnikova O, Sachchidanand , Sanchez R, Zeleznik-Le NJ, Ronai Z, Zhou MM: **Structural mechanism of the bromodomain of the coactivator CBP in p53 transcriptional activation.** *Mol Cell* 2004, **13(2):**251-263.
46. Singh M, Popowicz GM, Krajewski M, Holak TA: **Structural Ramification for Acetyl-Lysine Recognition by the Bromodomain of Human BRG1 Protein, a Central ATPase of the SWI/SNF Remodeling Complex.** *Chembiochem* 2007, **8(11):**1308-1316.
47. Shen W, Xu C, Huang W, Zhang J, Carlson JE, Tu X, Wu J, Shi Y: **Solution structure of human Brg1 bromodomain and its specific binding to acetylated histone tails.** *Biochemistry* 2007, **46(8):**2100-2110.
48. Lian LY, Barsukov IL, Sutcliffe MJ, Sze KH, Roberts GC: **Protein-ligand interactions: exchange processes and determination of ligand conformation and protein-ligand contacts.** *Methods Enzymol* 1994, **239:**657-700.